Two electrodeposition strategies for the morphology-controlled synthesis of cobalt nanostructures

Pier Giorgio Schiavi, Antonio Rubino, Pietro Altimari, and Francesca Pagnanelli

Citation: AIP Conference Proceedings **1990**, 020005 (2018); doi: 10.1063/1.5047759
View online: https://doi.org/10.1063/1.5047759
View Table of Contents: http://aip.scitation.org/toc/apc/1990/1
Published by the American Institute of Physics

Two Electrodeposition Strategies for the Morphology-Controlled Synthesis of Cobalt Nanostructures

Pier Giorgio Schiavi[1, a)], Antonio Rubino[1], Pietro Altimari[1], Francesca Pagnanelli[1]

[1] *Department of Chemistry, Sapienza University of Rome, P.le A. Moro 00185 Rome (IT)*
[a)] Corresponding author: piergiorgio.schiavi@uniroma1.it

Abstract. In this contribution, two different strategies are discussed to synthesize cobalt nanostructures: direct cobalt electrodeposition on a planar aluminum electrode and cobalt electrodeposition into nanoporous alumina templates generated by aluminum anodization (template electrodeposition). In the direct electrodeposition of cobalt on aluminum, cobalt nanoparticles are formed during the early stage of electrodeposition, which causes the depletion of cobalt ions near the electrode. Water reduction then takes place catalyzed by electrodeposited cobalt nanoparticles, which increases the pH near the electrode and can induce cobalt hydroxide precipitation. By varying the electrode potential and the cobalt ion concentration, the interplay between electrochemical growth of cobalt and water reduction could be controlled to induce transition from cobalt hexagonal nano-platelets to nanostructured films composed of cobalt nanoparticles and cobalt hydroxide nano-flakes. Cobalt nanowires can be synthesized by electrodeposition into nanoporous alumina templates generated by aluminum anodization. This approach typically involves the application of alumina templates produced by a two-step anodization procedure: the alumina nanoporous layer generated by a first anodization is dissolved in a chromic acid solution while a very ordered alumina nanoporous layer is produced by a second anodization stage. In accordance with previous studies, this procedure is fundamental to achieve uniform filling of the nanopores in the subsequent electrodeposition stage. In the present study, uniform filling of the nanoporous alumina generated by one-step anodization could be achieved by the electrodeposition of cobalt nanowires. This result was made possible by the application of a novel pulsed electrodeposition strategy.

1. INTRODUCTION

Cobalt nanostructured materials has attracted interest in a wide range of applications including, for example, lithium ion batteries electrodes [1], heterogeneous catalysis [2] and elctrocatalysts for water splitting reaction [3]. As well known, in any application, the achieved performances are largely influenced by the morphology, size, and surface number density of the cobalt nanostructures. This has generated a considerable interest towards the development of techniques for the controlled synthesis of metal nanostructures. Compared to solution phase methods, electrodeposition can enhance the controllability of nanostructure morphology, size and surface number density by tuning electrodeposition parameters. Major advantages of electrodeposition if compared to alternative technologies, including, for example, lithography and chemical vapor deposition, are reduced costs, increased versatility and easier scalability of the synthesis. Electrodeposition becomes a particularly attractive synthesis method when the immobilization of nanostructures onto conductive substrates is required. In this case, is possible, to synthesize the nanostructures and support it in only one step, using the catalytic support as working electrode for the deposition. Furthermore, reduced costs are mainly determined by the possibility to attain the deposition of the metal nanostructures in a unique step without any preparatory action, while versatility is determined by the large range of morphologies that can be generated by varying the operating parameters, mainly potential (or current density) and electrochemical bath's composition.

In this contribution, two different strategies are discussed to synthesize cobalt nanostructures: direct cobalt electrodeposition on a planar aluminium electrode and cobalt electrodeposition into nanoporous alumina templates

NANOINNOVATION 2017
AIP Conf. Proc. 1990, 020005-1–020005-7; https://doi.org/10.1063/1.5047759
Published by AIP Publishing. 978-0-7354-1706-9/$30.00

generated by aluminum anodization (template electrodeposition). This study on aluminium electrode was aimed for developing a novel synthesis route for supported catalyst on commercial aluminium foams. With this synthesis technique, design, control and scale-up of cobalt nanostructures production can be done easier and faster than the classical methods for catalysts preparation currently used.

2. MATERIALS AND METHODS

2.1 Direct Cobalt Electrodeposition on Aluminum Electrode

Cobalt electrodeposition on aluminum electrode was performed as reported in our previous work [4]. Briefly, analytical grade (Sigma-Aldrich ReagentPlus®) $CoSO_4 \cdot 7H_2O$, Na_2SO_4 and H_3BO_3 were used to prepare solutions with Co^{2+} concentration equal to 0.01M, 0.1M and 0.2M. Na_2SO_4 and H_3BO_3concentrations equal to 1 M and 0.5 M, respectively, were used in any solution. H_3BO_3 was used to buffer the pH increase induced by the co-reduction of water and protons. H_3BO_3 was employed to enlarge the range of cobalt ion concentration preventing the precipitation of cobalt hydroxide. In absence of H_3BO_3, cobalt hydroxide was precipitated during the early stage of electrodeposition starting from cobalt ion concentration around 0.01 M. The addition of H_3BO_3 can in contrast shift the precipitation to larger cobalt ion concentration. The variation of the cobalt ion concentration can thus be exploited to modify the characteristics of cobalt nanoparticles that are formed in absence of hydroxide precipitation.
A three-electrode jacketed glass cell without agitation was employed to perform any electrodeposition test. A spiral Pt wire and aluminum foil with surface equal to 0.5 cm^2 (Alfa Aesar 99%, 0.25 mm thickness) were the counter and the working electrode, respectively. An Ag/AgCl saturated electrode was used as reference electrode. Potential values reported throughout the manuscript are referred to the latter electrode. Before any electrodeposition test, the employed aluminum electrode was etched for 10 minutes in 1M NaOH and was then immersed for 15 minutes in 1M HNO_3.
Electrodeposition tests were performed by the Ivium-Stat potentiostat. The Lauda-ECO-RE-620-S thermostat with accuracy of ±0.01 °C was used to maintain constant electrolyte temperature at 25 °C in any experiment.
Potentiostatic electrodeposition was performed by maintaining the working electrode at constant potential. Electrolyte solutions with Co^{2+} concentration equal to 0.1 M and 0.2M were employed in these experiments.
Experiments were performed under potentiostatic electrodeposition at cathodic potential equal to -1.025V, -1.150V, -1.250V, -1.400V. The duration of any experiment was determined by imposing the overall transferred electric charge. Increasing the transferred charge at prescribed potential and concentration increased the duration of the experiment.

2.2 Cobalt Electrodeposition Into Nanoporous Alumina Templates

Cobalt electrodeposition into nanoporous alumina templates was performed as reported in our previous work [5]. Briefly, anodization tests were performed with aluminium foils (Alfa Aesar 99% - 1% Si + Fe, 0.25 mm thickness - annealed) with area exposed to the electrolyte equal to 1 cm^2. The employed aluminium foil was electropolished before anodization. Electropolishing tests of different durations and potentials were performed with a solution of 1:4 $HClO_4$ 60%wt : CH_3CH_2OH. Both electropolishing and anodization tests were performed in a two-electrode jacketed cell with a constant temperature of 0 ± 0.2 °C.
The anodic alumina oxide (AAO) templates were produced by one-step anodizations of different duration performed in a 0.3 M H_2SO_4 solution with an applied potential (U) of 25 V. In order to improve the electrical conductivity of the alumina template, at the end of any anodization, the cell potential was step-wise decreased every 30 seconds.
Nanowire electrodeposition tests were performed in a magnetically stirred three electrode jacketed glass cell at constant temperature of 35 ± 0.2 °C. A 25x20 mm Pt gauze and the AAO template were the counter and the working electrode, respectively. An Ag/AgCl saturated electrode was used as reference electrode. Potential values reported throughout the manuscript are referred to the latter electrode. The Watts bath, composed of 320 g/L $CoSO_4$ $7H_2O$ (Sigma Aldrich ≥ 99,0%), 45 g/L $CoCl_2$ $6H_2O$ (Sigma Aldrich ≥ 99,0%); 45g/L H_3BO_3 (Sigma Aldrich ≥ 99,5%) was employed to perform cobalt electrodeposition.
The electrodeposition includes the cyclic application of two elementary blocks signal. In the first block, the potential is maintained at the cathodic value of -8V for 10 ms. In the second following block the current is stepped to zero. Zero current is maintained for 2000 ms following which the cycle is repeated.
The cyclic application of the described elementary block with constant potential was cycled for the desired charge passing through the cell. Another electrodepostion method was used (Nielsch method). This method was implemented for the first time by Nielsch et al. [14] and successively adopted by other authors. This method, which employs the

same bath and electrodeposition temperature that were employed in the present work, allowed achieving uniform nickel deposition into alumina templates produced by double-step anodization. In the Nielsch method, electrodeposition is carried out by cycled application of an elementary block including three different pulses. Initially, the metal is deposited by applying a constant current pulse (70 mA cm−2) for 8 ms. Then, a second pulse with opposite polarity and constant potential is used for 2 ms to discharge the barrier layer capacitance. Finally, the cycle is closed by imposing zero current over a period ranging from 0.5 to 10 s to restore the metal ion concentration at the deposition interface.
The transferred charge required to achieve a prescribed length L of cobalt nanowires was estimated by the Faraday law under the assumption of 100% cobalt reduction faradaic efficiency, which gives $Q=(2FLS\rho)/M$ with F, S, ρ and M denoting the Faraday constant, the surface of the AAO electrode covered by nanopores, the density of the metallic cobalt and its molecular weight, respectively.

2.3 Characterizations of nanostructures

Field emission scanning electron microscopy (FE-SEM, Zeiss Auriga) was employed to characterize the morphology of cobalt nanoparticles onto aluminium foil, nanoporous alumina and cobalt nanowires. Focused ion beam (FIB, Orsay Physics - Cobra Ga column) was employed to exfoliate and generate cross sections of the alumina template filled by cobalt nanowires. This allowed evaluating the uniformity of filling. The chemical composition of the deposits was analyzed by energy dispersive X-ray spectroscopy (EDX, Bruker QUANTAX 123 eV). The software ImageJ was used to analyze SEM images of the deposits.

3. RESULTS AND DISCUSSION

3.1 Direct Cobalt Electrodeposition on Aluminium Electrode

During the direct electrodeposition of cobalt nanostructures onto aluminium working electrode, the effect of the applied potential to the working electrode and the effect of cobalt ion concentrations on nanostructures morphology was investigated. In order to quantify the effect of the above mentioned experimental parameters, the effect of each parameter was estimated taking constant the other one.

3.1.1 Effect of Applied Potential.

Figure 1. shown the effect of applied potential taking constant the overall charge transferred (10.6 mC) with Co^{2+} 0.1M.
Increasing the applied potential to the working electrode, increase the nanoparticles number density as reported from Table 1. In accordance with the theory of electrocrystallization, the increase of the electrode potential can increase the nucleation rate and the saturation number density of active sites [6, 7].

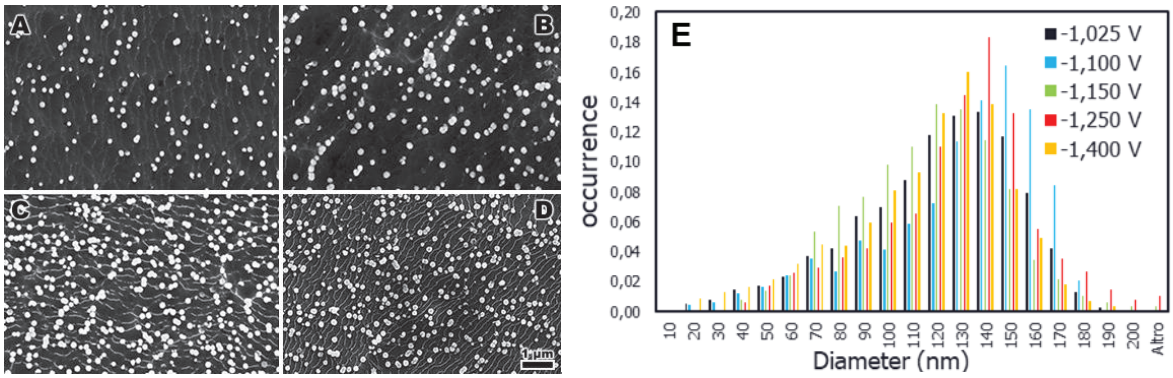

FIGURE 1. SEM images obtained from 0.1M Co^{2+} and 10.6 mC: A) -1.025V; B) -1.150V; C) -1.250V; D) -1.400V. E) nanoparticles mean diameter distribution.

On the other hand, was found that the nanoparticles mean diameter (Fig.1-E, Tab.1) did not vary within the selected potential range. In accordance with the Faraday law, since the charge transferred was kept constant, the increase of nanoparticles number density should, in contrast, lead to a decrease of nanoparticles mean diameter. A possible explanation to this result can be found on the simultaneous reduction of proton and water at the working electrode during the cobalt electrodeposition. In fact, it must be noted that a portion of the recorded transferred charge is attributable to water and proton reduction current. Based on the reported results, this effect can be due to an increase of the cobalt reduction rate after the increase of the working electrode potential, while, the reduction rate of proton and water was constant for the investigated potential range.

TABLE 1. Average diameter and number density of cobalt nanoparticles electrodeposited under potentiostatic operation. *E* is electrode potential, *md* is the average particle diameter, *s* is the diameter standard deviation, *nd* is the number density.

E [V]	md [nm]	s [nm]	nd [np/m^2]
-1.025	116	30	7.5×10^{12}
-1.100	124	30	7.5×10^{12}
-1.150	111	30	1.0×10^{13}
-1.250	123	30	1.3×10^{13}
-1.400	110	30	1.6×10^{13}

The electrodeposition of cobalt from all the reported condition lead to a cobalt electronucleation with a closely packed hexagonal morphology as shown from high magnification sem image (Fig.2). Hexagonal plane nucleation is a non-preferential nucleation route respect planar trapeze electronucleation route where cobalt grows towards solution bulk [8, 9].

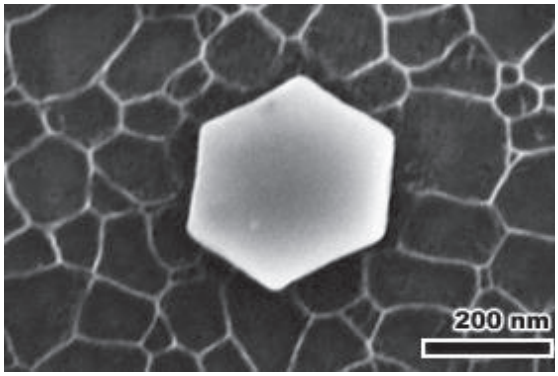

FIGURE 2. SEM images obtained from 0.1M Co^{2+} and 10.6 mC and -1.40

3.1.2 Effect of Cobalt Concentration

Increasing the cobalt ion concentration from 0.1M to 0.2M, for all the above mentioned applied potential, the morphology of the electrodeposited nanostructures changes from hexagonal nanoplatelets to nanoflakes as shown in Fig.3. These result from precipitation of cobalt hydroxide induced by the local pH increase. The increase of pH was determined by water and proton reduction taking place simultaneously with the cobalt electrodeposition. The formation of cobalt nanoflakes evidences the onset of cobalt hydroxide precipitation.

It is important to remark that the addition of H_3BO_3 enlarged the range of cobalt ion concentration that can prevent the precipitation of cobalt hydroxide. In absence of H_3BO_3, cobalt hydroxide was precipitated during the early stage of electrodeposition starting from cobalt ion concentration around 0.01 M. The addition of H_3BO_3 can in contrast shift the precipitation to larger cobalt ion concentration. The variation of the cobalt ion concentration can thus be exploited to modify the characteristics of cobalt nanoparticles that are formed in absence of hydroxide precipitation [10].

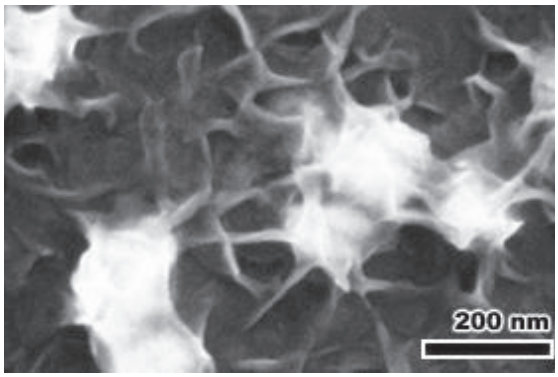

FIGURE 3. SEM images obtained from 0.2M Co^{2+} and 10.6 mC and -1.40

3.2 Cobalt Electrodeposition Into Nanoporous Alumina Templates

Anodization experiments were carried out in sulphuric acid solution with anodization conditions that, as described in previous studies [5, 11], allow optimal results in terms of nanoporous structure ordering.

As well known, a barrier oxide layer at the bottom of each pore characterizes any template produced by aluminium anodization. The barrier layer has high electrical resistance and thus electrically isolates the underlying aluminium from the electrodeposition bath. A decrease in the barrier layer resistance was achieved by a barrier layer thinning (BLT) procedure. This electrochemical treatment was conducted, with the same anodization condition, at the end of any potentiostatic anodization experiments. During the BLT treatment the anodization potential was step-wise reduced following an exponential law [12, 13]. The decrement of the applied potential lead to a decrease of the aluminium oxide formation rate through the application of anodic potential to the aluminum electrode. On the other hand, the dissolution rate, of the formed aluminum oxide through the acidic electrolyte solution, was kept constant. The effect of this treatment results in a dissolution of the oxide layer at the bottom of each nanopores. Because of this, exceeding with the decrease of the anodization potential, during the BLT treatment, lead to a detachment of the alumina template from the metallic aluminum electrode [5]. This BLT technique, resulted in the formation of tree-like alumina nanopores that improved the electrical contact between the metal and the electrodeposition bath [5]. Furthermore, it must be observed that pore etching treatment, which is performed at the end of anodization, contributes to thin the barrier layer at the bottom of the pores and thus to increase the overall electrical conductivity.

The as obtained anodic alumina template was employed as working electrode for cobalt nanowires electrodeposition. In contrast to what found with AAO templates produced by doublestep anodization by Nielsch et al. [14] , not uniform pore filling was achieved (Fig.4-A).

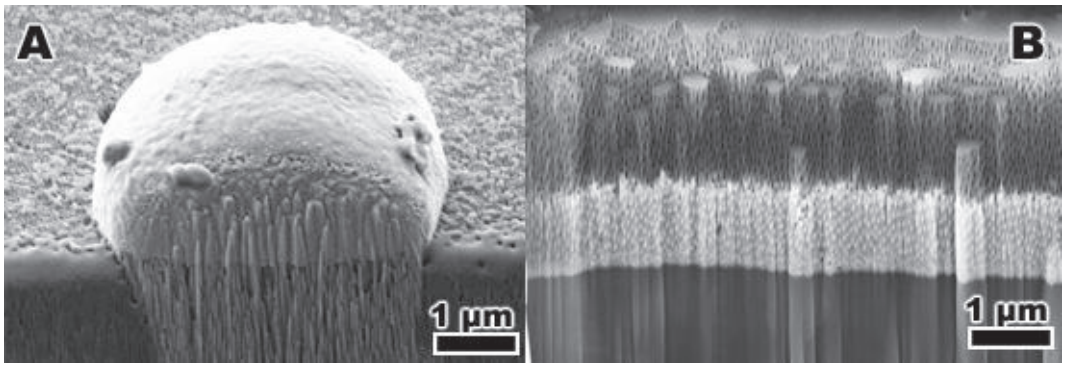

FIGURE 4. FIB cross-sectional SEM images of electrodeposited cobalt (light grey in figure) into anodic aluminium oxide. A) electrodeposition following Nielsch method; B) Electrodeposition by implemented electrodeposition method.

The nucleation and growth of cobalt nanowires only in some pores lead to the spillover of cobalt nanowires above the alumina template, with the appearance of cobalt hemispherical deposits. It must be remarked, that a transferred charge

$Q=(2FLS\rho)/M$ was imposed in the performed experiment with the prescribed length L lower than the length of the nanopores obtained during the aluminium anodization.

Complete pore filling and narrow length distribution could, in contrast, be reached with the electrodeposition method described in section 2.2. In this latter experiment, uniform nucleation and growth of cobalt nanowires at the bottom of nanopores removed the occurrence of cobalt spill over, which ensured the disappearance of cobalt clusters above alumina surface. Results illustrated in Fig.4-B evidence that uniform pore filling and narrow nanowire length distribution can be attained with AAO templates produced by the illustrated one-step anodization procedure if large cathodic values close to −8 V (during Nielsch method a cathodic potential of about -1.5V was applied) are imposed to the alumina working electrode template.

Large cathodic potential lead to an increase in the nucleation rate and the saturation number density of active sites. Furthermore, the application of large cathodic potentials should be required in presence of an oxide to enable charge transfer, the required cathodic potential increasing with increasing the thickness of oxide layer. In accordance with this latter hypothesis, different charge transfer rates would be expected at the bottom of the nanopores depending on the thickness of the barrier layer. This effect would be particularly pronounced at potential values insufficient to achieve tunneling. On the other hand, as reported in our previous work [5], the inhomogeneous distribution of the barrier layer does not generate an inhomogeneous distribution of the charge transfer rate among the nanopores. In fact, an uniform fill of the template with narrow nanowires length distribution was found cycling the electrodeposition with -8 V, to form nanowires just with a length equal to 50 nm, and afterwards cycling the electrodeposition with an applied potential of -1.5 V. It can thus be derived that the application of -8.0 V during the initial cycles enabled the nucleation at the bottom of all the pores and that the successive application of the cathodic potential of -1.5 V was sufficient to sustain the uniform growth of nanowires. It then follows that the resistance to charge transfer determined by the inhomogeneous distribution of the barrier layer cannot explain the satisfactory filling uniformity attained at potentials equal to -8 V. Particularly, narrower nanowire length distribution attained with increasing the cathodic potential might be attributed to the transition from progressive to instantaneous nucleation [5]. In fact, in accordance with the theory of electrocrystallization, increasing the electrode potential can increase the nucleation rate and the saturation number density of active sites available for metal nucleation [7, 15, 16].

4. CONCLUSIONS

Cobalt electrodeposition on a planar aluminum electrode allow production of cobalt nanostructures including hexagonal nanoplatelets, and cobalt hydroxide nanoflakes. Under potentiostatic electrodeposition, hexagonal nanoplatelets with sharp corners were formed with cobalt ion concentration lower than 0.2 M. Morphology, size distribution and number density of the nanoplatelets were influenced by the imposed potential. The average size of nanoplatelets could be controlled by modification of the overall transferred charge. Increasing the cobalt ion concentration to 0.2 M caused transition from hexagonal nanoplatelets to cobalt nanoflakes. Nanoflakes were formed by precipitation of cobalt hydroxide. The precipitation was induced by the pH increase that accompanies the reduction of water catalysed by cobalt nanoparticles.

Cobalt electrodeposition into nanoporous alumina templates generated by aluminum anodization ensure the formation of ordered cobalt nanowires array. Our analysis demonstrates, in contrast to what reported by previous studies, that improved filling attained by increasing the electrode potential is determined by the transition from progressive to instantaneous nucleation. In accordance with this result, we demonstrate that the application of large cathodic potentials is required to enforce uniform filling during the early stage of electrodeposition. The illustrated results can provide a valuable contribution to the development of methodologies for large-scale synthesis of metallic nanowires,

AKNOWLEDGEMENTS

The authors greatly acknowledge the staff of Centre for Nanotechnology Applied to Engineering of Sapienza Univertiy of Rome (CNIS) for the SEM measurement.

REFERENCES

1. L. Zhan, S. Wang, L.-X. Ding, Z. Li and H. Wang, Journal of Materials Chemistry A **3** (39), 19711-19717 (2015).
2. Q. Liu, X. Guo, J. Chen, J. Li, W. Song and W. Shen, Nanotechnology **19** (36), 365608 (2008).
3. L. Liao, Q. Zhang, Z. Su, Z. Zhao, Y. Wang, Y. Li, X. Lu, D. Wei, G. Feng and Q. Yu, Nature nanotechnology **9** (1), 69-73 (2014).
4. P. G. Schiavi, P. Altimari, F. Pagnanelli, E. Moscardini and L. Toro, in *Chemical Engineering Transactions* (2015), Vol. 43, pp. 673-678.
5. P. G. Schiavi, P. Altimari, A. Rubino and F. Pagnanelli, Electrochimica Acta **259**, 711-722 (2018).
6. F. Pagnanelli, P. Altimari, M. Bellagamba, G. Granata, E. Moscardini, P. G. Schiavi and L. Toro, Electrochimica Acta **155**, 228-235 (2015).
7. A. Milchev, *Electrocrystallization: fundamentals of nucleation and growth*. (Springer Science & Business Media, 2002).
8. D. Grujicic and B. Pesic, Electrochimica acta **49** (26), 4719-4732 (2004).
9. H. Nakano, K. Nakahara, S. Kawano, S. Oue, T. Akiyama and H. Fukushima, Journal of applied electrochemistry **32** (1), 43-48 (2002).
10. P. G. Schiavi, P. Altimari, R. Zanoni and F. Pagnanelli, Electrochimica Acta **220**, 405-416 (2016).
11. G. D. Sulka, Nanostructured materials in electrochemistry **1**, 1-116 (2008).
12. W. Cheng, M. Steinhart, U. Gösele and R. B. Wehrspohn, Journal of Materials Chemistry **17** (33), 3493-3495 (2007).
13. C. Sousa, D. Leitao, M. Proenca, A. Apolinario, J. Correia, J. Ventura and J. Araujo, Nanotechnology **22** (31), 315602 (2011).
14. K. Nielsch, F. Müller, A.-P. Li and U. Gösele, Advanced Materials **12** (8), 582-586 (2000).
15. P. Altimari and F. Pagnanelli, Electrochimica Acta **206**, 116-126 (2016).
16. P. Altimari and F. Pagnanelli, Electrochimica Acta **205**, 113-117 (2016).